**RESEARCH ARTICLE**

# Stiffness modeling of thermoset polymer fibers

**Israel Greenfeld** ⓘ | **Mark Shneider** ⓘ | **Antonia Kaestner** ⓘ | **H. Daniel Wagner** ⓘ

Department of Molecular Chemistry and Materials Science, Weizmann Institute of Science, Rehovot, Israel

**Correspondence**
Israel Greenfeld, Department of Molecular Chemistry and Materials Science, Weizmann Institute of Science, Rehovot 76100, Israel.
Email: green_is@netvision.net.il

**Funding information**
Israel Science Foundation, Grant/Award Number: #2439/19; G.M.J. Schmidt Minerva Centre of Supramolecular Architectures at the Weizmann Institute; Harold Perlman family

**Abstract**
Recent progress in creating micro and nano-scale thermoset polymer fibers through extensional flow reveals remarkable mechanical properties. For instance, epoxy microfibers display a notable increase in stiffness, strength, and toughness as their diameter decreases. This size-dependent behavior, well-explored and explained in thermoplastic polymers, is far from being understood in thermoset polymers, as their densely cross-linked network structure seems to restrain preferential directionality. Our theoretical analysis proposes that, during the pre-gel curing phase, when the thermoset polymer begins clustering but remains in a liquid state, substantial cluster elongation is induced by the extensional flow. This elongated formation persists to some extent after curing completion, resulting in enhanced mechanical properties along the fiber's primary axis. Concurrently, the high extension reduces fiber diameter, leading to a power-law diameter dependence of fiber stiffness. The model agrees well with experimental data from tensile tests on epoxy microfibers, highlighting the potential to fine-tune mechanical properties by controlling the curing process, and laying the groundwork for future improvements.

**KEYWORDS**
electrospinning, epoxy, extensional flow, fiber, mechanical drawing, polymer, stiffness, thermoset

## 1 | INTRODUCTION

Thermosetting polymers are obtained by curing a liquid resin, a process that creates irreversible, covalent bonds (crosslinks) between monomers. Unlike thermoplastic polymers, in which long chains are not crosslinked but rather reversibly entangled, thermosets cannot be melted or shaped after curing. The massive crosslinking creates a 3D network that percolates throughout the cured material, making thermosets strong, hard and stiff, as well as high-temperature resistant and chemically resilient.[1] At the same time, most thermosets are brittle and prone to fracture as a result of their rigidity, requiring reinforcement by strong fibers for load-bearing applications. A thermoset of wide industrial importance is epoxy, with applications ranging from structural and engineering adhesives to electronics encapsulation, protective coatings, films, and sealing; epoxy is used in aircrafts and satellites as a composite matrix reinforced by glass and carbon.[2,3]

Recent application of extensional flow in creating micro and nano-scale thermoset polymer fibers revealed remarkable mechanical properties. For instance, epoxy microfibers exhibit a significant increase in stiffness, strength, and toughness when

their diameter is progressively decreased.[4–9] In particular, these fibers become ductile and can elongate more than twice their length without breaking, implying an intrinsic structural rearrangement at the nano or molecular scale. Sometimes called size-dependence, because below a certain critical size the material properties grow steeply, this phenomenon has been widely explored in a variety of materials. Size dependence in thermoplastic nanofibers has been studied and several models were suggested, including surface tension, confinement, molecular orientation, crystallinity, and density grading.[10,11] By contrast, in thermosets, size dependence has been scarcely investigated and is little understood.

The study of thermoset micro and nanofibers produced by extensional flow is fairly new, applying techniques such as electrical drawing (electrospinning) and mechanical drawing (pulling) of polymer solution or neat resin. To the best of our knowledge, no attempt has been made to model the molecular conformation of such fibers. The elongation of thermoplastic polymers under extensional flow has been broadly investigated, using the concepts of linear flexible chains, confining tube, chain reptation, and chain stretching and retraction.[11–20] The general polymer behavior is similar in thermosets, consisting of stretching of chains under the stresses induced by an extensional flow, followed by partial retraction due to the elastic forces in chains, which relieves some of the stress and achieves a new state of equilibrium.[21–25] However, the two polymer types are quite different, and therefore their modeling differs. Thermoset polymers are not linear but randomly branched and chemically reactive, they are not entangled but instead are at overlap concentration near the gel point, and therefore the notions of confining tube and chain reptation do not apply.

In this study, we suggest a model based on the molecular rearrangement induced by extensional flow, dependent on the polymer extent of reaction (curing). We show that above a certain critical strain rate, the branched polymer sharply elongates, causing an increase in molecular alignment. This elongation tends to rearrange polymer clusters from their arbitrary dispersion to sequential order. We further show that, after some relaxation and final curing, the fiber stiffness (elastic modulus) is proportional to the strain rate applied during the flow. The high extension also squeezes the fiber diameter, leading to an inverse-square power law dependence of the stiffness on diameter. The stiffness model compares well with recent experimental results. Aspects of the drawing technique and tuning of parameters are discussed.

## 2 | THERMOSET POLYMER CONFORMATION INDUCED BY EXTENSIONAL FLOW

### 2.1 | Gelation process

Monomers of a thermoset polymer resin gradually bond to each other during a curing process, to form clusters resembling branching trees. Branching occurs when reacted polymer chain sections cross-link to one another by bonding. A class of thermoset polymers are epoxy resins, whose monomers have epoxide end-groups which react with hardeners like polyfunctional amines, creating strong cross-links with other epoxy monomers. The clusters grow steadily as the curing process proceeds, until the gel point is reached, when a first infinite cluster percolates through the entire system. The gel point marks the transition of the polymer solution from liquid state to solid state. When the gel point is approached, while the polymer solution is still fluid, the clusters are at overlap concentration (marginal overlap) with their finite-size neighbors, but not deeply overlapped as that would result in chemical reaction making a larger cluster. Our interest is in modeling the polymer conformation in that state when subjected to extensional flow, using the critical percolation model.[26]

The cross-linking progress is defined by the extent of reaction $p$, the fraction of bonds already formed out of the maximum possible, ranging from zero to unity. In a branched polymer without loops, $p$ signifies the probability of bonds being created from a parent site placed on a tree lattice. Given the chemical functionality of the polymer, $f$, the average number of new bonds per parent monomer is $p(f-1)$, excluding the bond to its own grandparent. For the polymer to keep growing to infinity, this value should be greater than unity, $p(f-1) > 1$, so that each new generation has more members on average, otherwise only finite-size polymers will be created. Thus, the transition to infinite growth occurs at the critical extent of reaction which marks the gel point[26,27]:

$$p_c = \frac{1}{f-1}. \tag{1}$$

At the gel point $p = p_c$, meaning that at each parent site one bond on average is reacted out of $f-1$ possible bonds, so that some parent sites are bonded to one or more child monomers while some have not yet reacted (Figure 1D). An example is a system with one type of functional group, enabling reaction between bifunctional (e.g., an epoxy monomer) and trifunctional (e.g., an amine hardener) species. At a stoichiometric ratio of
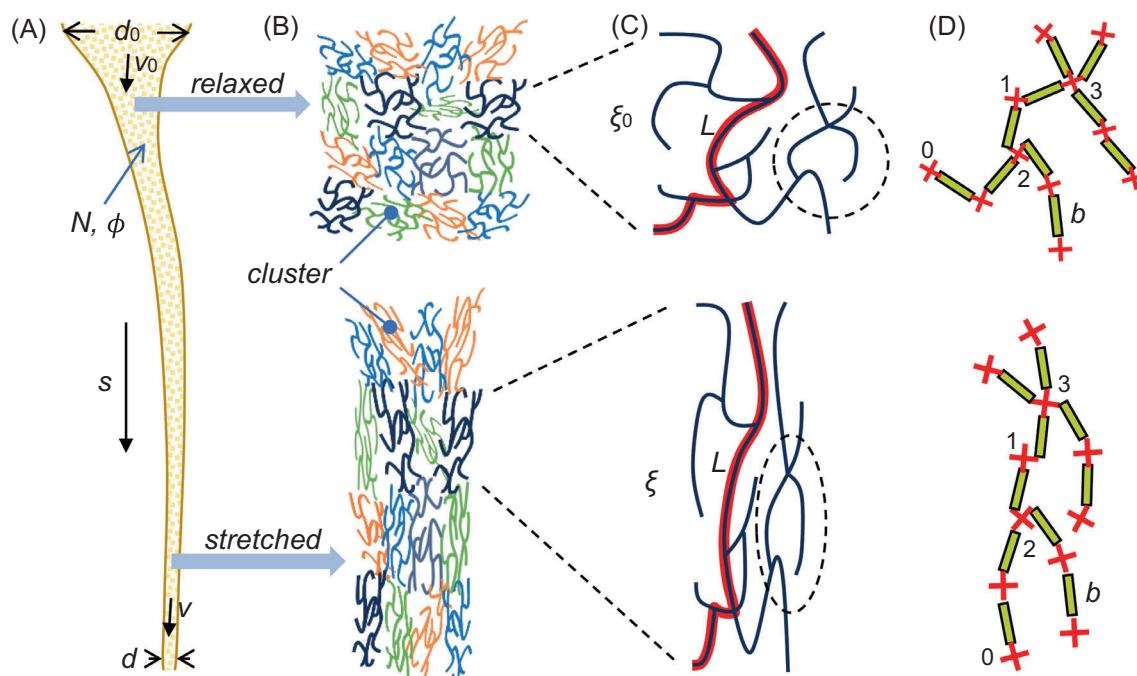
**FIGURE 1** Illustration of polymer cluster conformation in extensional flow. (A) Polymer solution at concentration $\phi$ and polymerization degree $N$, under extensional flow of downstream strain rate $s$, velocity $v$, and diameter $d$. (B) Branched polymer chains (clusters) at rest (relaxed—top) and during high extension (stretched—bottom). Each chain is colored differently, and is at overlap concentration with its neighbors (not strongly overlapped). (C) A cluster of size (correlation length) $\xi_0$ at rest (top, of order $10^1$ nm) and $\xi$ during extension (bottom). $L$ (red curve) is a typical contour length between two distant end points on a cluster. (D) Schematic molecular conformation (detail), for polymer with functionality $f = 4$ (represented by 4-arm crosslinker, red X), showing partially and fully reacted monomers (typical number of reacted child bonds is indicated at each site). The monomers are represented by rectangles, where $b$ is the monomer length.

about three epoxy monomers to one triamine monomer ($f \cong 4$), $p_c \cong 0.33$ compared to the value of 0.31 identified by viscosity measurements of epoxy solutions.[9] $p_c$ may be different for more complex chemical systems, which are not discussed here because the effect is just a correction to the value of $p_c$.

A key parameter which governs the scaling laws is the relative extent of reaction, defined as:

$$\varepsilon \equiv \frac{p - p_c}{p_c} = (f - 1)p - 1, \tag{2}$$

and is related to the characteristic degree of polymerization $N$ (sometimes denoted by $N^*$) by:[26]

$$N \approx 2\frac{f - 2}{f - 1}|\varepsilon|^{-1/\sigma} \approx |\varepsilon|^{-2.22}, \tag{3}$$

where the critical exponent $\sigma = 0.45$.[26] The prefactor for $f = 4$ is 1.33, close to unity. The ($\approx$) symbol denotes a scaling relationship, where constants of order unity are omitted. As $\varepsilon$ is negative in the pre-gel domain, the absolute value is used. Thus, the number of monomers in a cluster, $N(\varepsilon)$, depends on the reaction progress and diverges to infinity at the gel point ($\varepsilon = 0$). $N$ is an important variable for determining the solution rheological behavior, and consequently the polymer conformation in extensional flow. The critical percolation model assumes close packing of monomers on a lattice, a state not kept when the polymer is diluted by solvent, but the critical exponents remain of the same type.[12]

The extent of reaction $p$ depends on the reaction type, temperature and time. Typically, the curing process of a thermoset polymer goes through intermediate reactants before reaching the final product (consecutive reaction), and therefore the rate of $p$ starts slow and increases with time.[28,29] For instance, in epoxy during pre-gel curing, $p$ depends roughly quadratically on the time,[9] and can be approximated by $p(t) \cong k^2(T)t^2$ ($p \ll 1$), where $t$ is the time from curing start and $k(T)$ is Arrhenius temperature factor.[30] The relative extent of reaction in such a process would be (Equation 2):

$$\varepsilon = \frac{p(t)}{p(t_c)} - 1 \cong \left(\frac{t}{t_c}\right)^2 - 1, \tag{4}$$

where, $t_c$ is the time from curing start to the gel point. Although the rate of the reaction $p$ increases with temperature, $\varepsilon$ is independent of temperature.

## 2.2 | Cluster size and relaxation time

The size of a polymer cluster at rest, prior to applying an extensional load, is given by its correlation length, $\xi_0$ (Figure 1C), determined by the balance between the entropic contraction and the excluded volume repulsion between monomers[26]:

$$\xi_0 \approx bN^{1/\mathcal{D}} \approx b|\varepsilon|^{-\nu} \sim |\varepsilon|^{-0.88}, \tag{5}$$

assuming the excluded volume is equal to the monomer volume. $b$ is the Kuhn monomer linear length, $\mathcal{D} = 2.53 \cong (d+2)/2$ is the fractal dimension of a branched polymer in spatial dimension $d = 3$, $1/\mathcal{D} = 0.40$, and $\nu = 1/\mathcal{D}\sigma$ is a critical exponent expressing the size divergence. For instance, the size of an epoxy branched cluster of $10^3$ monomers is of order 20 nm. The branched cluster at the pre-gel phase is tenuous, with monomers volume fraction of $b^3 N/\xi_0^3 \approx N^{1-3/\mathcal{D}} \approx N^{-0.19}$ (e.g., 0.28 at $N = 1000$), but still much more compact compared to linear chains ($N^{-0.76}$).

A parameter needed for defining the cluster relative extension under load is the maximum possible extended cluster length $L$ (Figure 1C, red line), which in linear chains is simply $bN$. To estimate $L$, the chain section along the $L$-path may be approximated by a freely-jointed linear real chain. Thus, $\xi_0 \approx bn^{\tilde{\nu}}$, where $n$ is the average number of monomers along the $L$-path, and $\tilde{\nu} \cong 0.588$ is Flory's exponent.[26,31,32] Equating with Equation (5), we obtain $n \approx N^{1/\tilde{\nu}\mathcal{D}} \approx N^{0.67}$ and therefore the maximum extended cluster length scales as:

$$L = bn \approx bN^{1/\tilde{\nu}\mathcal{D}} \approx b|\varepsilon|^{-1/\tilde{\nu}\mathcal{D}\sigma} \sim |\varepsilon|^{-1.49}. \tag{6}$$

The elasticity of viscoelastic liquids, such as resins of thermoset polymers, is time-dependent so that the stress induced by an applied extension decays over time. The decaying rate is governed by the polymer relaxation time, $\tau$, that is the time it takes for a stretched polymer to return to its equilibrium conformation at rest. This characteristic time depends on the polymer size, $\xi_0$ or $N$, on the monomer hydrodynamic friction coefficient, and on the hydrodynamic interaction between the polymer and its surrounding liquid. These dependencies differ between diluted and non-diluted resins, as shown ahead.

In case the polymer resin is not diluted (neat resin), because molecules at overlap concentration are space-filling with no topological interactions, hydrodynamic interactions are partially screened, and the relaxation time of a cluster may be approximated by the Rouse model[26,33]:

$$\tau \approx \frac{\varsigma N}{kT}\xi_0^2 \approx \tau_0 N^{1+2/\mathcal{D}} \approx \tau_0|\varepsilon|^{-(1/\sigma+2\nu)} \sim |\varepsilon|^{-3.98} \text{ neat resin,} \tag{7}$$

where, $\tau_0 \approx \varsigma b^2/kT$ is the relaxation time of a single monomer ($\varsigma$ is the monomer friction coefficient, $k$ is Boltzmann constant, and $T$ is the temperature). $\tau_0$ is the time a standalone monomer would diffuse a distance of its own size. Given the polymer resin viscosity $\eta_r$, the monomer friction coefficient is $\varsigma \approx \eta_r b$ (Stokes law), and the monomer relaxation time is $\tau_0 \approx \eta_r b^3/kT$.

In case the polymer is dissolved in solvent, as is done when producing fibers by electrospinning,[7,9] hydrodynamic screening may no longer be assumed because the polymer drags solvent, monomers and small clusters entrapped in its pervaded volume, and therefore the Zimm model is more applicable[12,26,34]:

$$\tau \approx \frac{\varsigma \xi_0}{bkT}\xi_0^2 \approx \tau_0 N^{3/\mathcal{D}} \approx \tau_0|\varepsilon|^{-3\nu} \sim |\varepsilon|^{-2.64} \text{ solution.} \tag{8}$$

The overall friction term $\varsigma N$ (Equation 7) is replaced by $(\varsigma/b)\xi_0$ to reflect the friction of the whole polymer cluster instead of the cumulative friction of all monomers. The resin viscosity $\eta_r$ will be that of the resin dissolved in solvent.

Determining the monomer friction coefficient $\varsigma$ in either case is not straight-forward: (i) *without solvent* (neat resin), the monomers will sense the viscosity of the liquid resin, which might be quite high but fairly stable throughout the pre-gel curing process when most of the monomers are not yet bonded; for example, typical viscosity of epoxy resin is of order 0.1–10 Pa s RT,[35] and the Kuhn monomer length is ~1.4 nm (very close to the chemical monomer length of ~1.3 nm),[36] resulting in $\tau_0 \sim 10^{-7} - 10^{-5}$ s; (ii) *with solvent* (solution), the cluster will sense the viscosity of the solvent mixed with monomers and small clusters, which might vary as the curing progresses; for example, the viscosity of a solution of epoxy dissolved in 80% solvent was measured to be 0.003 Pa s RT,[9] but quickly increased to 0.2 Pa s closer to the gel point, resulting in $\tau_0 \sim 10^{-9} - 10^{-7}$ s. However, when the polymer dilution is sufficiently high (but not too high to cause precipitation and segregation which may quench gelation),[12] we may assume the cluster senses just the fairly stable viscosity of the solvent surrounding it, as most of the monomers are unreacted or in small clusters. Evidently, the relaxation time $\tau$ is much faster in the presence of solvent, because $\tau_0$ is lower and the exponent of $N$ is smaller. In practice, the relaxation time $\tau$ might follow the range between the Rouse and Zimm models.[34]

## 2.3 | Cluster elongation

Consider a branched polymer under extensional flow with a constant velocity gradient (strain rate) $s = \nabla v$, a condition fairly fitting both mechanically[5] and electrically[7,11,37] drawn fibers (Figure 1A). The cluster is stretched affinely with the flow (Figure 1B), with a subsequent relative extension defined by:

$$\epsilon \equiv \frac{\xi}{L}, \tag{9}$$

where, $\xi$ is the stretched size and $L$ is the maximum extension possible (Equation 6) (Figure 1C,D). Because stretching is affine with the flow, a polymer section between any pair of monomers in a branched polymer is stretched by the same relative extension $\epsilon$. The cluster elongates at a rate of $\dot{\xi} = \xi s$, so that its relative extension rate is $\dot{\epsilon} = \dot{\xi}/L = \epsilon s$. The extension induces a net elastic force $\Delta f$ (dimensionless), which tends to retract the cluster back to relaxed state within the relaxation time $\tau$ (Equation 7 or 8), at a retraction rate of $-\Delta f/\tau$. After a short duration, the cluster stretching and retraction reach equilibrium:

$$\Delta f = f(\epsilon) - f(\epsilon_0) \approx s\tau\epsilon, \tag{10}$$

where, $\epsilon_0$ is the extension at rest, and $f(\epsilon)$ is the elastic force at extension $\epsilon$. The term $s\tau$ represents the instantaneous stiffness of the cluster, a competition between two time scales, that of the strain rate and that of the relaxation.

The retraction force $f$ represents the polymer entropic elasticity: at small extension, the force is derived from the elastic free energy of a branched polymer, $\mathcal{F} \approx \frac{3kT\xi^2}{2bL}$,[32,38] so that the force $F = \frac{\partial \mathcal{F}}{\partial \xi} \approx \frac{3kT}{b}\frac{\xi}{L}$, and in dimensionless form $f \approx \frac{b}{kT}F \approx 3\frac{\xi}{L} \approx 3\epsilon$, a linear dependence on the extension; at high extension, as chain conformations become less probable, the force rises sharply by a nonlinear function such as $\frac{1-\epsilon_0}{1-\epsilon}$.[11,16,20] Thus:

$$f \approx 3\epsilon\frac{1-\epsilon_0}{1-\epsilon}. \tag{11}$$

The relative extension at rest is given by (Equations 5 and 6):

$$\epsilon_0 = \frac{\xi_0}{L} \approx N^{1/\mathcal{D}-1/\tilde{\nu}\mathcal{D}} \approx |\varepsilon|^{-\nu+1/\tilde{\nu}\mathcal{D}\sigma} \approx |\varepsilon|^{0.62}. \tag{12}$$

The exponent of $N$ is $-0.28$. Other representations of the force nonlinear rise are known,[11,20] affecting the solution of the stretching equation (Equation 10) and the

resulting rise of the extension; however, the general trend of rising extension at high stretching is not affected.

The stretching equation bears similarity in form to the stretching of entangled linear polymer chains.[11,20] However, the thermoset polymer size and its relaxation time are completely different: $\xi_0 \sim N^{0.4}$ (compared to $\sim N^{0.6}$), $L \sim N^{0.67}$ (compared to $\sim N$), and $\tau \sim N^{1.8 \text{ or } 1.2}$ (compared to $\sim N^3$), being much more compact and with faster relaxation. The difference stems from the dissimilar physical state of the two polymer types. The thermoset clusters are randomly branched polymers, which, in critical percolation close to the gel point, are space-filling but non-interacting with their neighbors, a state termed hyperscaling.[26] By contrast, thermoplastic chains are linear and therefore larger, and, at sufficiently high concentration, create an entangled network with their neighbors. The relaxation of a cluster is by diffusing a distance of its own correlation size, without topological constraints. By contrast, a linear chain diffuses a distance of its own stretched (primitive) length by reptating between the topological constraints posed by the network, a process which takes longer.

The solution of Equation (10) for the full range of $s\tau$ (below and above the stretching transition) is presented in the Appendix A (Equation A2) and depicted in Figure 2. The relative extension exhibits a sharp transition at a critical strain rate $s_c = 3/\tau$ (or $s/s_c = s\tau/3$), where the extension starts rising steeply with increasing strain rate. The extension in that region may
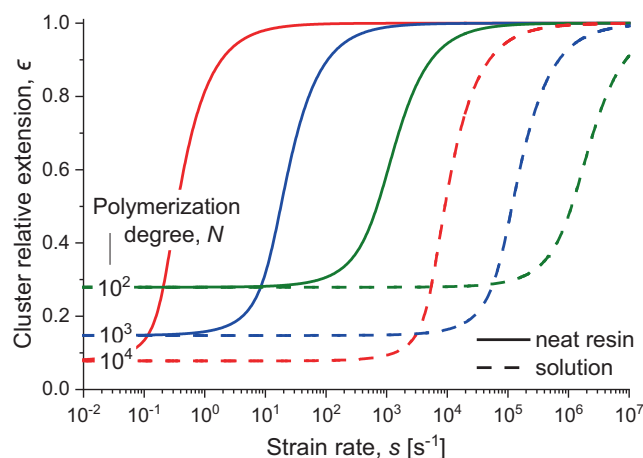


**FIGURE 2** Polymer cluster extension. Log-linear trend plots of the relative extension $\epsilon$ (Equation A2) versus the extensional flow strain rate $s$. The characteristic degree of polymerization is $N = 10^2, 10^3, 10^4$, corresponding to relative extent of reaction $|\varepsilon| = 0.143, 0.051, 0.018$ (polymer functionality $f = 4$). Depicted for neat resin (polymer without solvent, solid lines) and solution (polymer with solvent, dashed lines). The cluster relaxation time $\tau$ is given by Equations (7) and (8), with $\tau_0 = 10^{-6}, 10^{-8}$ s, respectively, and the initial extension $\epsilon_0$ is given by Equation (12).

be approximated by neglecting the force at rest (Equation 10, $f(\epsilon_0) \ll f(\epsilon)$):

$$\epsilon \approx 1 - \frac{3(1-\epsilon_0)}{s\tau} \approx 1 - \frac{1-\epsilon_0}{s/s_c}, \ s \gg s_c. \qquad (13)$$

The stretching transition occurs at a lower strain rate when the degree of polymerization is higher (longer relaxation time) as a result of a more progressed extent of reaction. The transition occurs at a higher strain rate when the polymer is dissolved in solvent (faster relaxation time). Therefore, for the purpose of achieving high extension and molecular orientation, higher strain rates are required when producing fibers from solutions, compared to neat resin. The strain rate may be normalized by the critical strain, making the plot in Figure 3A universal, with just a single parameter—the degree of polymerization $N$, which represents the extent of reaction.

At the transition point, the equilibrium between stretching and retraction shifts from small extension to high extension, which increases the retracting force significantly. The critical strain rate is given by (Equations 7 and 8):

$$s_c \equiv \frac{3}{\tau} \approx \frac{3}{\tau_0} \begin{cases} N^{-(1+2/\mathcal{D})} \approx |\varepsilon|^{1/\sigma+2\nu} \approx |\varepsilon|^{3.98} & \text{neat resin} \\ N^{-3/\mathcal{D}} \approx |\varepsilon|^{3\nu} \approx |\varepsilon|^{2.64} & \text{solution,} \end{cases} \qquad (14)$$

depicted in Figure 3B. The exponent of $\varepsilon$ is positive, implying that when the gel point is approached ($\varepsilon \to 0$),

the critical strain rate tends to zero. Fiber drawing is typically performed close to the gel point (large $N$), to ensure strength and continuity of the flow,[5,7,9] meaning that the extension transition may start at a relatively low strain rate. This is a positive outcome, because high molecular extension and orientation are a desirable conformation in terms of the fibers' mechanical properties, as will be elaborated further on.

The extension calculated in this section applies to large clusters with a characteristic degree of polymerization $N$, as defined in Equation (3). However, near the gel point, the system consists of a highly polydisperse distribution of polymers,[26] a mixture of large clusters, small clusters, and unreacted monomers. Small clusters and monomers have very fast relaxation times because of their low degree of polymerization (Equations 7 and 8), and therefore their extension will not be retained even under very high strain rates. Thus, the system may simultaneously contain highly stretched large polymers and relaxed small polymers and unreacted monomers. The overall molecular orientation is affected accordingly.

## 2.4 | Molecular orientation

The cluster extended conformation induced by the flow is accompanied by partial molecular alignment of its monomers in the flow direction. The molecular orientation can be estimated by placing the cluster on a 3D Cartesian
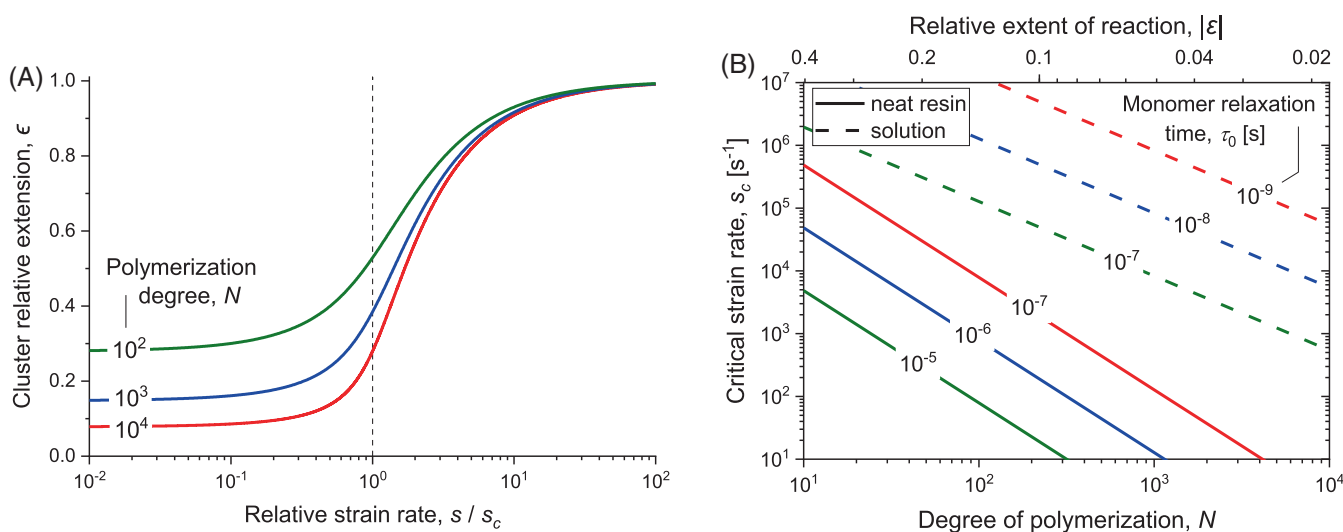


**FIGURE 3** Polymer cluster normalized extension and critical strain rate. (A) Universal log-linear trend plot of the relative extension $\epsilon$ (Equation A2) versus the extensional flow strain rate $s$ normalized by the critical strain rate $s_c$ (Equation 14). The characteristic degree of polymerization is $N = 10^2, 10^3, 10^4$, corresponding to relative extent of reaction $|\varepsilon| = 0.143, 0.051, 0.018$ (polymer functionality $f = 4$). Applies to both neat resin (polymer without solvent) and solution (polymer with solvent). The stretching transition occurs at $s = s_c$, denoted by the dashed vertical line. (B) Log–log trend plot of the critical strain rate $s_c$ (Equation 14) versus the degree of polymerization $N$, for neat resin and solution, for a range of monomer relaxation time $\tau_0$. The relative extent of reaction $|\varepsilon|$ relating to $N$ (Equation 3) is shown in the top horizontal axis.

lattice,[26] and assigning the probability $P_i^{\pm}$ ($i = x, y, z$) that a monomer will be aligned with each of the six possible directions.[11,20] $x$ is the flow longitudinal axis, whereas $y$ and $z$ are the lateral axes. The $(+)$ and $(-)$ signs indicate the positive and negative directions of each axis, respectively. The force induced by the flow in each direction is assumed uniform throughout the cluster, and therefore the associated probability is uniform as well.

The molecular orientation in a stretched cluster is calculated by Hermans' orientation parameter, $O_s = \frac{3}{2}\langle\cos^2\theta\rangle - \frac{1}{2}$, where $\theta$ is the angle a monomer forms with the flow direction $x^+$, and $\langle\cos^2\theta\rangle$ is an average over all $N$ monomers. $O_s$ is zero for arbitrary monomer orientations and unity for full alignment with $x$. Assigning the probability $P_i^{\pm}$ and angle $\theta_i^{\pm}$ to each direction, $O_s = \frac{3}{2}\sum\left(P_i^{\pm}\cos^2\theta_i^{\pm}\right) - \frac{1}{2}$, where the summation is over all six directions. This equation is simplified noting that in a Cartesian lattice $\theta_y^{\pm} = \theta_z^{\pm} = \frac{\pi}{2}$ and $\theta_x^{\pm} = 0$, yielding the monomers orientation in a stretched cluster:

$$O_s = \frac{3}{2}\left(P_x^+ + P_x^-\right) - \frac{1}{2}. \tag{15}$$

The orientation is irrespective of the positive or negative direction of $x$, as both directions contribute to orientation. This is not the case with the relative extension, because the positive direction contributes to elongation by a fraction $P_x^+$, whereas the negative direction subtracts from it by a fraction $P_x^-$, and therefore:

$$\epsilon = \epsilon_x = P_x^+ - P_x^-. \tag{16}$$

This result applies to large clusters, whereas the contribution of small clusters and unreacted monomers to orientation is negligible because of their fast relaxation. The weight fraction of large clusters may be approximated by the extent of reaction $p$, because near the gel point these clusters are dominant in size; in other words, the critical weight-average degree of polymerization of all clusters is similar to the characteristic degree of polymerization $N$. Using this approximation, the overall molecular orientation in the polymer mixture is given by:

$$O \cong O_s p \cong O_s p_c, \tag{17}$$

where, near the gel point, $p$ is estimated by the critical extent of reaction $p_c$. The maximum theoretically achievable overall orientation is $p_c$, about 0.33 for functionality $f = 4$ (Equation 1), compared to 1 (full orientation) achievable in thermoplastic polymers with linear chains.

Using the expressions for $O_s$ and $\epsilon$, and the monomers direction probabilities, the orientation solution for the full range of $s\tau$ (below and above the stretching transition) is presented in the Appendix A (Equation A8) and depicted in Figure 4 versus the relative strain rate $s/s_c = s\tau/3$. At high stretching, beyond the extension transition, the cluster's dominant monomer direction is determined by the probability $P_x^+$ in the positive stretching direction, whereas $P_x^-$ in the opposite direction is negligible. Substituting $P_x^+ \cong \epsilon$ and $P_x^- \cong 0$, the orientation is approximated by (using Equation 13 for $\epsilon$):

$$O \cong \left(\frac{3}{2}\epsilon - \frac{1}{2}\right)p_c \approx \left[1 - \frac{3(1-\epsilon_0)}{2s/s_c}\right]p_c, \ s \gg s_c. \tag{18}$$

The orientation in this strain rate region is linearly dependent on the extension, and rises steeply with $s\tau$. Written in terms of the gelation progress (Equations 12 and 14):

$$O \approx \left[1 - \frac{9(1-N^{-0.28})}{2s\tau_0 N^x}\right]p_c, \ s \gg s_c, \tag{19}$$

where the exponent $x = 1 + 2/\mathcal{D} \cong 1.79$ for neat resin and $x = 3/\mathcal{D} \cong 1.19$ for solution. $N$ can be expressed in terms of the relative extent of reaction $\varepsilon$ (Equation 3). As the curing process draws closer to the gel point $(\varepsilon \to 0, N \to \infty)$, the cluster molecular orientation approaches full alignment of monomers with the flow direction, and the overall orientation approaches $p_c$.
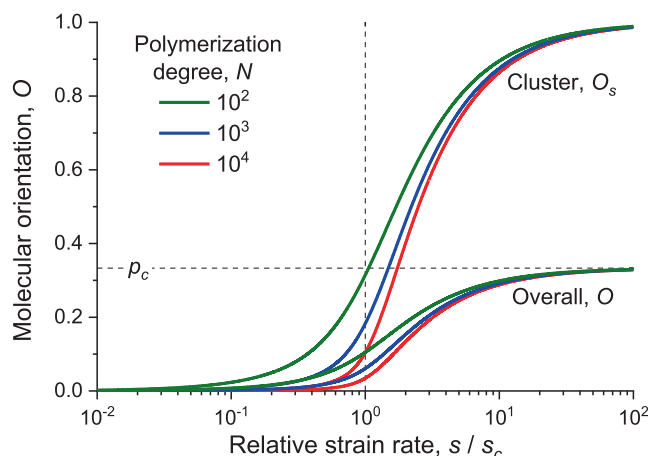


**FIGURE 4** Overall and cluster molecular orientation. Log-linear trend plots of the overall molecular orientation $O$ and the cluster molecular orientation $O_s$ (Equations 17 and A8) versus the extensional flow strain rate $s$ normalized by the critical strain rate $s_c$ (Equation 14). The characteristic degree of polymerization is $N = 10^2, 10^3, 10^4$, corresponding to relative extent of reaction $|\varepsilon| = 0.143, 0.051, 0.018$ (polymer functionality $f = 4$). The stretching transition occurs at $s = s_c$, denoted by the dashed vertical line. The maximum achievable overall orientation is given by the critical extent of reaction, $p_c = 1/3$ ($f = 4$).

The polymer cluster experiences a sharp transition from low to high molecular orientation, which occurs at the critical strain rate $s_c$. Large clusters can achieve very high orientation (up to 1) at high strain rates, but as their weight fraction in the system is only about $p_c$, and the contribution of small clusters and unreacted monomers to orientation is negligible, the maximum achievable overall orientation is equal to $p_c$. Fibers are created when the polymer state is near the gel point but still fluid, and therefore some relaxation of stretched molecules may occur until the gel point is finally reached ($p = p_c$), but the general orientation trend is likely retained. Beyond the gel point, large clusters become part of an infinite network and their relaxation is mostly inhibited, whereas small clusters and monomers can still diffuse and bond, completing the polymer curing ($p \to 1$). The high polydispersion of clusters and their low weight fraction near the gel point limit the orientation degree that can be obtained in thermoset polymers by extensional flow, compared to thermoplastic polymers. Molecular orientation measurements of solid fibers are therefore expected to be fairly low, but a measured overall value $O$ may imply a much higher cluster orientation of $O_s \cong O/p_c$.

Polarized Raman Spectroscopy of as-prepared epoxy fibers (diameters 8–20 μm), mechanically drawn from neat liquid resin, showed a low molecular orientation index of about 0.1 along the fiber axis at penetration depth of 5–10 μm.[8] Similar tests of such fibers (diameter 120 μm), conducted at NEST in Pisa, also showed negligible orientation index at the fiber center; however, a scan across the fiber showed gradual rising of the index toward the fiber surface up to a significant value of 0.3–0.35, which might indicate nonuniform molecular rearrangement. In both test campaigns, necked fibers produced by mechanical drawing of solid fibers exhibited substantial molecular orientation indices of 0.5–0.75. Raman depth scan of necked epoxy fibers exhibited uniform molecular orientation along the fiber radius, but no such test was done for as-prepared fibers.[8] Further polarized Raman molecular orientation measurements of as-prepared electrospun epoxy fibers of smaller diameters are in progress; preliminary results of 2 μm fibers demonstrate an average index of 0.45, equivalent to $O = 0.35$ which implies high cluster orientation.

## 2.5 | Supramolecular structure

The described gelation process is reflected in the polymer solid structure: in critical percolation close to the gel point, large branched clusters are space-filling but noninteracting with their neighbors; beyond the gel point, further curing generates crosslinks between clusters.

Experimental studies of bulk epoxy have shown that its morphology at nanoscale is inhomogeneous, exhibiting a nodular structure with a characteristic globular size of 15–45 nm.[39–42] The nodule size is of the same order as typical polymer clusters near the gel point (Equation 5). Although such morphology sometimes appears in thermoplastic polymers as well, these studies attribute the nodular structure to the curing chemistry of epoxy, and suggest high covalent bonding density inside the nodules but lower density in the matrix outside the nodules. Furthermore, correlation was established between nodule size and ultimate mechanical properties, plastic flow, and crack initiation and arrest.[41] At the gel point, large crosslinked microgels (clusters), which are too massive to diffuse, come into contact with neighboring microgels and form crosslinks at their interfaces, creating a nonhomogeneous network.[42] More recent studies of drawn epoxy fibers show low orientation in as-prepared fibers, but high orientation in necked fibers, suggesting reorientation of the bridging molecular regions between nodules due to plastic deformation.[5,8] This experimental evidence considered, it is evident that the clusters formation during gelation and their size account for the nodular structure observed after solidification and curing.

The stretched conformation of large clusters has an important impact on the nodular structure of the solid fiber. The cluster shape is oblong, elongated by a factor $\epsilon/\epsilon_0$ in the fiber axis direction, and shrunk by a factor $\sqrt{\epsilon/\epsilon_0}$ in the lateral directions (assuming constant cluster volume). This means that the density of unreacted branch ends (dangling bonds) at the cluster tips should be higher than at its sides. At rest, the probability that the end of an unreacted branch will be oriented in any outward direction is 1/6. At high strain rate, the probability that an end will be oriented longitudinally is about $P_x^+ \cong \epsilon \approx 1 - (1 - \epsilon_0)\left(\frac{s}{s_c}\right)^{-1}$ (Equations 13 and 16); in the absence of external force in the lateral directions, half of the unreacted branches are oriented inward while the other half outward, and therefore the probability that an unreacted branch will be oriented sideward (laterally) is $\frac{1 - P_x^+}{2} \approx \frac{1}{2}(1 - \epsilon_0)\left(\frac{s}{s_c}\right)^{-1}$. This means that the bonding rate at the edge of a stretched cluster is significantly higher than at its sides, increasing the likelihood that clusters will bond to each other in the fiber direction.

A numerical example may clarify this: suppose we measure (e.g., by Polarized Raman Spectroscopy)[8] an overall fiber orientation of 0.2, which corresponds to about $\frac{s}{s_c} \cong 3$, implying cluster orientation of about $0.2/p_c \cong 0.6$ (Figure 4, $N = 10^3$). Then, the longitudinal probability is about 0.7 ($\epsilon_0 \cong 0.15$) whereas the lateral probability is about 0.14. In other words, the density of longitudinal unreacted end bonds is about 5 times higher, so that the likelihood of longitudinal bonding between

clusters is about 5 times higher than lateral bonding (see illustration in Figure 5D), and about 4.3 times higher than at rest. The cluster elongates by a factor of about 5 (Figure 3A) and shrinks by a factor of about $\sqrt{5}$, hence its aspect ratio is about 11, a rod-like shape. Plasma etching of the surface of bulk epoxy and epoxy fibers supports this suggestion (Figure 5A,C): while the nodular structure in bulk is isotropic, the fiber structure exhibits a connected elongated nodular, rod-like network oriented in the fiber longitudinal (stretching) direction.

The preferred longitudinal crosslinking between clusters may be retained to a large extent even after some relaxation of the clusters. So, the reorganization of inter-cluster bonds is imprinted in the network crosslinking structure, and may impact the elastic and plastic behavior of the solid matrix. The nodules (former clusters) might favor a sequential order, creating long chains of nodules, as illustrated in Figure 5D. This formation may translate into high stiffness, the focus of this study, as the connectivity of nodules in the direction of the fiber primary axis is high. It may also translate into high ductility, which is uncharacteristic of brittle thermoset polymers, as well as into high strength.[5,7] This is likely the result of the higher mobility of clusters compared to the omni-bonded bulk matrix (Figure 5D and 5B, respectively), as well as the alignment of chains to the fiber axis made possible by the greater drawing ratio (necked fibers).[8]
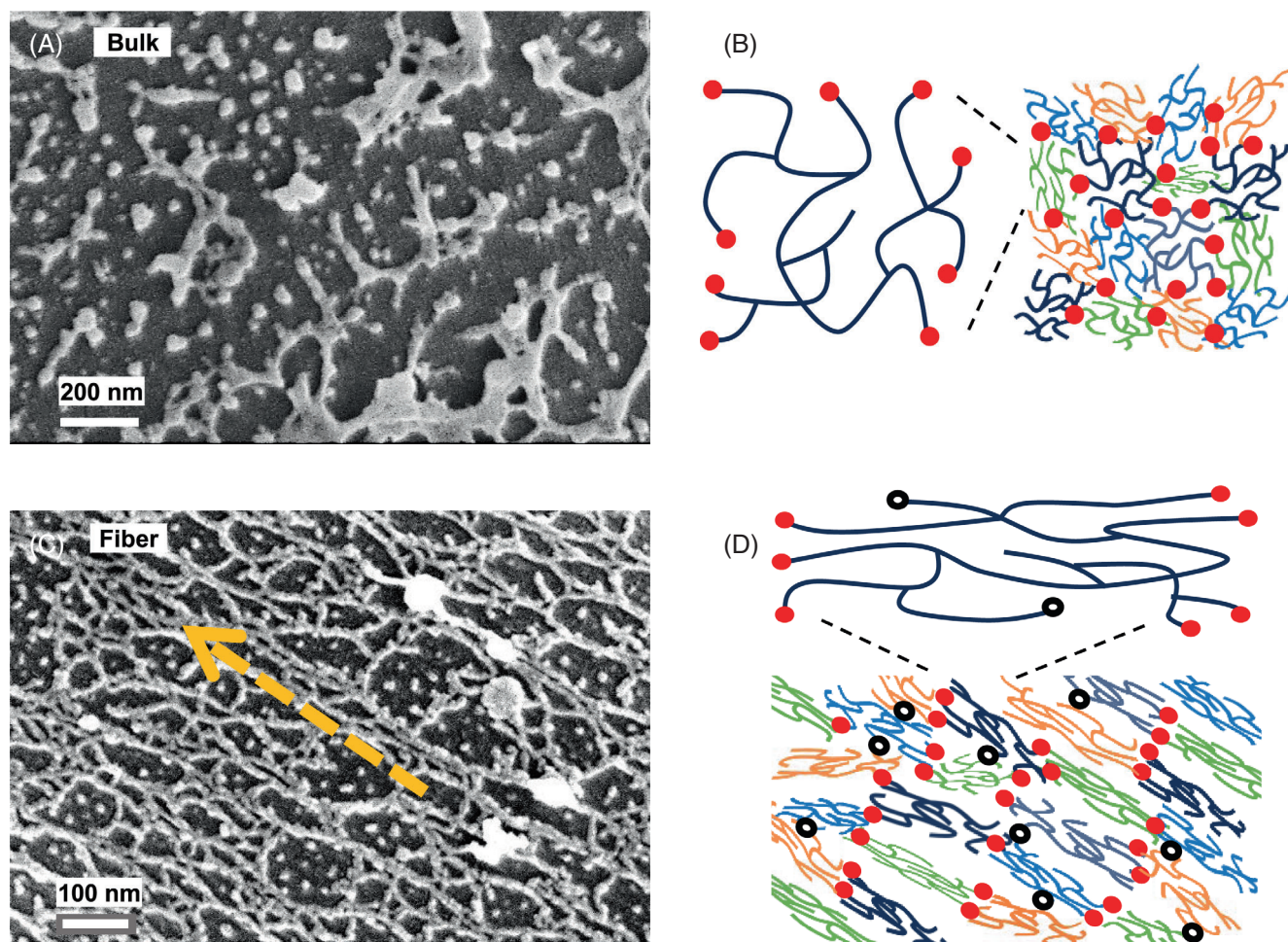


**FIGURE 5** Nodules elongation, directionality, and networking. (A, C) SEM images after plasma surface etching of bulk epoxy (top) and an electrospun epoxy fiber (bottom). Softer regions are etched deeper and appear black, whereas the nodules appear bright. The small bright dots are nodule heads protruding from a deeper layer. The stretched nodules in the fiber appear as a connected, elongated, rod-like network, oriented $-23° \pm 19°$ with respect to the image frame (0.85 goodness of fit), coincident with the fiber longitudinal (stretching) direction (orange arrow). The nodules area fraction in the bulk and fiber samples is 29% and 32%, respectively, compatible with $p_c \cong 0.33$. Etching in both samples was conducted at 3.5 SCCM oxygen flow STP, 40 W power, and duration of 12.8 min. The clusters direction and area fraction were measured by imageJ on thresholded images. (B) Illustration of a relaxed cluster with randomly distributed unreacted ends (red dots), and the matching network with randomly distributed crosslinks. (D) Illustration of a stretched cluster, with most unreacted ends distributed at its tips (red dots) and less at its sides (black circles), and the matching network with preferred crosslinking in the stretching direction.

# 3 | SOLID FIBER STIFFNESS

## 3.1 | Stiffness dependence on orientation

We first calculate the stiffness (in terms of the tensile elastic modulus) of a stretched cluster, and then estimate the overall stiffness as done for the orientation. The basic assumption is that, even though some chain relaxation takes place after the drawing process, the molecular conformation induced by the extensional flow is partially retained after solidification and final curing. We apply an aggregate model,[11,43,44] defining a monomer as a representative volume unit (RVE) with known axial modulus $E_1$ and lateral modulus $E_2$. $E_1$ represents the monomer backbone strong covalent bonding stiffness, and $E_2$ represents the monomer intermolecular bonding stiffness (mainly weak VDW and hydrogen bonds), where typically $E_1/E_2 \sim 10^2 - 10^3$.[11,45–47] This estimate is based on the relation $E = S/r_0$, where $S$ is the bond spring constant and $r_0$ is the atomic radius ("atom size")[46]: the spring constant of a covalent bond ranges within $20–200$ N/m, and that of a VDW bond ranges within $0.5–2$ N/m[46]; typical covalent radius is 76 pm and Van der Waals radius is 170 pm (Carbon).[46,48,49]

Given the average monomer orientation in a cluster, $O_s$ (Equation 15), and the related orientation probabilities, the cluster axial ($x$-direction) tensile modulus $E_s$ can be calculated using a plain iso-stress mixing rule (that is, uniform stress throughout the cluster). Iso-stress is more suitable than iso-strain for the stretching of a free chain section, along which the tension stress is uniform, analogous to a string of stiff and soft springs connected serially. For an applied axial stress $\sigma$, a monomer aligned with the fiber contributes a strain $\sigma/E_1$ in the $x$-direction, whereas a monomer aligned laterally contributes a strain of $\sigma/E_2$ in the $x$-direction. The overall strain is obtained by summing up the strain fractions using the corresponding alignment probabilities:

$$\frac{\sigma}{E_s} = P_x \frac{\sigma}{E_1} + (1 - P_x) \frac{\sigma}{E_2}, \tag{20}$$

where, $P_x \equiv P_x^+ + P_x^- = (1 + 2O_s)/3$ (inverting Equation 15). Extracting $O_s$ and rearranging, the longitudinal modulus is:

$$E_s = \frac{E_0}{1 - \alpha O_s}, \text{where } \alpha = \frac{2(E_1/E_2 - 1)}{2E_1/E_2 + 1} \cong 1, \tag{21}$$

where typically $E_1 \gg E_2$. The isotropic modulus (no molecular alignment) is:

$$E_0 = \frac{3E_1 E_2}{2E_1 + E_2} \cong \frac{3}{2} E_2, \tag{22}$$

dominated by the intermolecular stiffness. This approximation is obtained from Equation (20), using $P_x = 1/3$ and neglecting $E_2$ in the denominator as $E_1 \gg E_2$. Furthermore, substituting VDW bond stiffness $S = 0.5$ N/m and VDW atomic radius $r_0 = 170$ pm, the isotropic modulus is estimated by $E_0 \cong \frac{3}{2}\frac{S}{r_0} \cong 4.4$ GPa, in the ballpark of bulk thermoset polymers.[46] The maximum theoretically achievable cluster modulus occurs when $O_s = 1$, so that $E_s = E_0/(1 - \alpha) = E_1$.

The polymer morphology consists of a fraction $p \cong p_c$ of large stretched clusters which form an elongated network and a fraction $1 - p_c$ of amorphous polymer, resembling a fiber-reinforced composite where the connected elongated clusters are analogous to reinforcing fibers and the amorphous polymer is analogous to a matrix. Using a mixture rule fitting such a composite,[50] the overall modulus is given by:

$$E = E_s p_c + E_0 (1 - p_c) \cong E_0 \left[ \frac{p_c}{1 - \alpha O/p_c} + (1 - p_c) \right], \tag{23}$$

where, $O_s$ was substituted by $O/p_c$ (Equation 17), and $O$ is given in the Appendix A (Equation A8). The maximum theoretically achievable modulus is $E_1 p_c$ ($E_s = E_1 \gg E_0$). The stiffness solution for the full range of $s\tau$ (below and above the stretching transition) is depicted in Figure 6 versus the relative strain rate $s/s_c = s\tau/3$. At high stretching, beyond the extension transition, the stiffness may be approximated by (Equation 18):

$$E \approx E_0 \frac{2p_c}{3(1 - \epsilon_0)} \frac{s}{s_c}, \quad s \gg s_c, \tag{24}$$

where the constant $\alpha$ was approximated by 1. As $\epsilon_0 \approx N^{-0.28}$ (Equation 12) is weakly dependent on $N$, the prefactor of order unity may be omitted, and we may write a scaling rule for the modulus:

$$E \approx E_0 \frac{s}{s_c}, \quad s \gg s_c. \tag{25}$$

The modulus in this high stretching region is proportional to the flow relative strain rate. Written in terms of the gelation progress (Equations 14 and 3, omitting the prefactors):

$$E \approx E_0 s \tau_0 p_c \begin{cases} N^{1.79} \approx |\varepsilon|^{-3.98} & \text{neat resin} \\ N^{1.19} \approx |\varepsilon|^{-2.64} & \text{solution} \end{cases} \quad s \gg s_c. \tag{26}$$
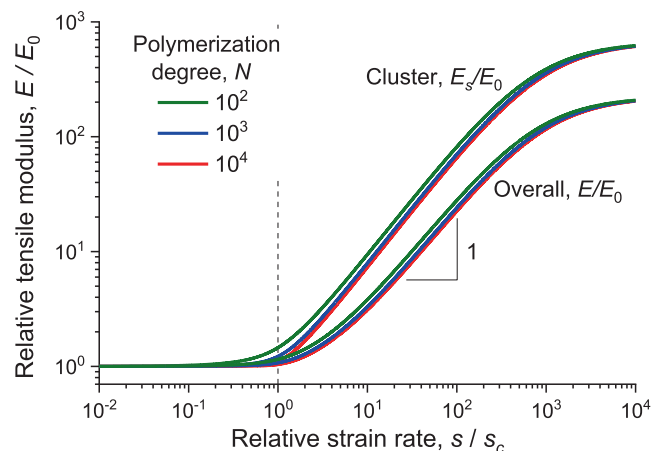
**FIGURE 6** Overall and cluster tensile stiffness. Log–log trend plots of the overall tensile modulus $E$ and the cluster modulus $E_s$ (Equation 23) normalized by the bulk modulus $E_0$, versus the extensional flow strain rate $s$ normalized by the critical strain rate $s_c$ (Equation 14). The characteristic degree of polymerization is $N = 10^2, 10^3, 10^4$, corresponding to relative extent of reaction $|\varepsilon| = 0.143, 0.051, 0.018$ (polymer functionality $f = 4$). The stretching transition occurs at $s = s_c$, denoted by the dashed vertical line. The modulus rise is nearly linear with the strain rate (power slope of $\sim 1$). The ratio between the monomer modulus and the intermolecular modulus is $E_1/E_2 = 10^3$, and the maximum achievable overall modulus is given by $E_1 p_c$ with critical extent of reaction $p_c = 1/3$.

Thus, the fiber overall modulus is linearly dependent on the strain rate, and is a power law of the characteristic degree of polymerization or equivalently the relative extent of reaction.

The fiber elastic stiffness rises steeply when the polymer resin is stretched at a high strain rate larger than the critical strain rate $s_c$, and the rise is in proportion to the strain rate. The dominant contribution to this rise is that of large clusters, which can approach the monomer stiffness at very high strain rates, but as their weight fraction in the system is only about $p_c$, the maximum achievable overall modulus is reduced accordingly. This limits the modulus increase that can be obtained in thermoset polymers by extensional flow, compared to thermoplastic polymers. The fiber modulus increases by a power law with the polymer resin relative extent of reaction at the time of its drawing. Some cluster relaxation may reduce the stiffness before the gel point is reached. Thus, processing the polymer as near the gel point as possible may yield stiffer fibers as well as lessen the relaxation effect.

## 3.2 | Stiffness dependence on diameter and critical diameter

In a volume-conserving extensional flow, the polymer diameter $d$ decreases with the inverse square root of the velocity $v$. The polymer diameter further decreases with the square root of the polymer volume fraction $\phi$ due to evaporation of the solvent (if diluted). Given the polymer initial diameter $d_0$ and initial drawing velocity (feedrate) $v_0$, the polymer diameter scales as[11,51]:

$$d \approx d_0 \left(\frac{\phi v_0}{v}\right)^{1/2} \approx d_0 \left(\frac{\phi v_0}{sl}\right)^{1/2}, \qquad (27)$$

substituting $v = sl$, the constant strain rate $s$ multiplied by the drawing distance $l$. Modulus transition occurs in fibers produced by a flow whose strain rate equals the critical strain rate $s_c$ (Equation 14), corresponding to a critical diameter (or crossover diameter):

$$d_c \approx d_0 \left(\frac{\phi v_0}{s_c l}\right)^{1/2} \approx d_0 \left(\frac{\phi v_0 \tau_0}{3l}\right)^{0.5} \begin{cases} N^{0.90} \approx |\varepsilon|^{-1.99} & \text{neat resin} \\ N^{0.59} \approx |\varepsilon|^{-1.32} & \text{solution,} \end{cases}$$
$$(28)$$

depicted in Figure 7B. The critical diameter is larger when the extent of reaction is higher, or, in other words, the modulus transition starts at a higher diameter when the polymer is closer to the gel point.

As the fiber diameter is inversely dependent on the square root of the strain rate, the fiber diameter scales as:

$$d \approx d_c \left(\frac{s}{s_c}\right)^{-1/2}. \qquad (29)$$

The stiffness solution for the full range of $d/d_c$ (below and above the stretching transition) is depicted in Figure 7A using the solution of Equation (23) with $s/s_c$ substituted by $(d/d_c)^{-2}$. Expressing the modulus at high stretching in terms of the diameter (Equations 24 and 25):

$$E \approx E_0 \frac{2p_c}{3(1-\epsilon_0)} \left(\frac{d}{d_c}\right)^{-2} \approx E_0 \left(\frac{d}{d_c}\right)^{-2}, \, s \gg s_c. \qquad (30)$$

we obtain a power law for the diameter dependence of the modulus. An approximation for the whole range of the strain rate is given by:

$$E \approx E_0 \left[1 + \frac{2p_c}{3(1-\epsilon_0)} \left(\frac{d}{d_c}\right)^{-2}\right], \qquad (31)$$

depicted in Figure 7A (dotted curves). This approximation converges to Equation (30) when $d \ll d_c$ and to $E \approx E_0$ when $d \gg d_c$, as required.

Starting at the critical diameter, the stiffness rises steeply with diameter decrease at a power of $-2$ seen in the universal plot in Figure 7A. The critical diameter has
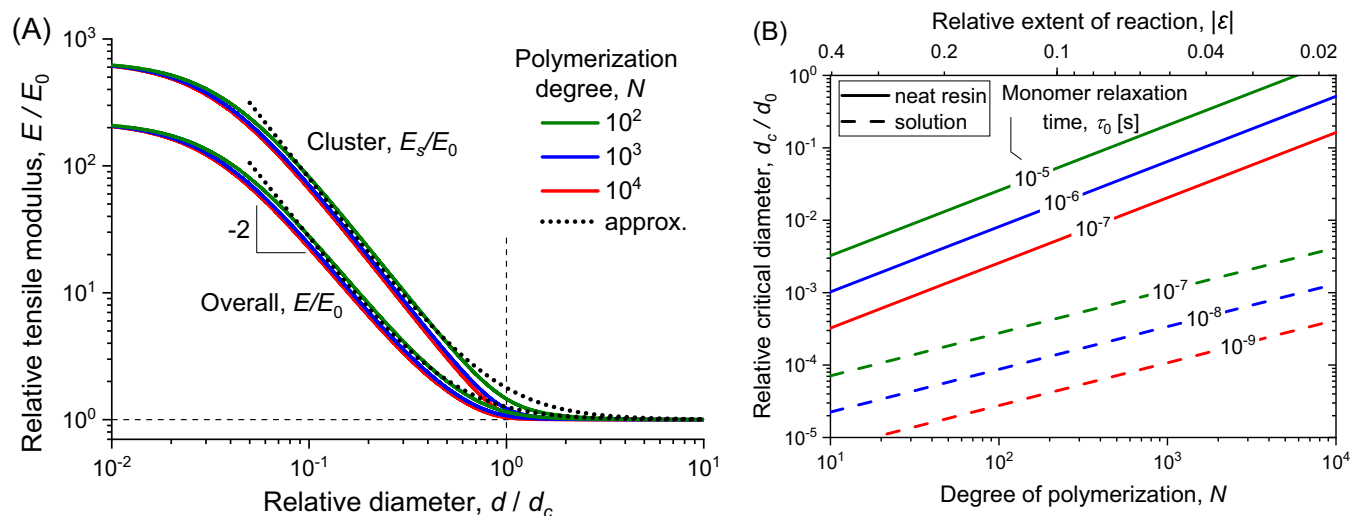
**FIGURE 7** Fiber tensile stiffness and critical diameter. (A) Log–log trend plots of the overall tensile modulus $E$ and cluster modulus $E_s$ (Equation 23) normalized by the bulk modulus $E_0$, versus the fiber diameter $d$ normalized by the critical diameter $d_c$. The characteristic degree of polymerization is $N = 10^2, 10^3, 10^4$, corresponding to relative extent of reaction $|\varepsilon| = 0.143, 0.051, 0.018$ (polymer functionality $f = 4$). The stretching transition occurs at $d = d_c$, denoted by the dashed vertical line. The modulus rises with the decrease in diameter at a power slope of $-2$. The ratio between the monomer modulus and the intermolecular modulus is $E_1/E_2 = 10^3$, and the maximum achievable overall modulus is given by $E_1 p_c$ with critical extent of reaction $p_c = 1/3$. Approximations are depicted by dotted curves (Equation 31). (B) Log–log trend plot of the critical diameter $d_c$ (Equation 28) versus the degree of polymerization $N$, for neat resin and solution, for a range of monomer relaxation time $\tau_0$. The relative extent of reaction $|\varepsilon|$ relating to $N$ (Equation 3) is shown in the top horizontal axis.

a power law dependence on the extent of reaction, with a positive exponent of the degree of polymerization, indicating that the stiffness rise starts earlier, at a larger diameter, as the process gets nearer the gel point. Also, the critical diameter depends on the solution and flow parameters, including polymer concentration, initial diameter, initial velocity, drawing distance, and monomer relaxation time. The latter parameter is viscosity dependent, so that the critical diameter is much smaller for a solution compared to a neat resin (Figure 7B). According to the suggested model, the stiffness is not directly impacted by the diameter. Rather, two independent processes are affected by the extensional flow—molecular alignment and diameter shrinkage. The molecular alignment, and consequently the stiffness, is proportional to the flow strain rate, whereas the diameter shrinkage is inversely proportional to the square root of the strain rate. Put together, we obtain the inverse-square power dependence of the stiffness on the diameter. This effect is sometimes termed *size dependence* or *size effect*, as the stiffness diameter-dependence is readily observable in mechanical tests, but this term is somewhat misleading because it disregards the role of the molecular conformation.

Experimental measurements of epoxy fibers elastic modulus are presented in Figure 8. These fibers were produced by extensional flow, either mechanically drawn (pulled) or electrically drawn (electrospun) from neat resin or solution with various solvents and concentrations. The data spans a wide range of diameters (see inset), depending on the solution composition and the drawing technique, and was therefore collapsed into a single plot by normalizing the diameter by the critical diameter. The trend of rising modulus with decreasing diameter is vindicated and agrees fairly well with the theoretical prediction (solid curves). The log–log plot (Figure 8B) demonstrates the power law of the modulus diameter-dependence. The data in each test group is somewhat dispersed because, unlike similar data of thermoplastic fibers,[11] the degree of polymerization $N$ is not stable due to the spontaneous continuation of the curing process during testing of a large number of samples. $N$ diverges quickly near the gel point: an uncertainty in $N$ by a factor of 1.5–2 causes a change in $d_c$ (Equation 28) of about $\pm 50\%$ (dashed curves).

The critical diameter values used to scale the modulus data of each test group (Figure 8 legend) are generally inline with the prediction of Equation (28): (i) The neat epoxy resin has indeed a much higher $d_c$ than that of the other groups which are diluted solutions, because of its higher concentration ($\phi = 1$) and larger exponent of the polymerization degree $N$. (ii) The $d_c$ of the pulled solutions is much higher than that of the electrospun solutions, because of larger initial diameter $d_0$ and shorter drawing length $l$. (iii) Solutions of the same solvent and drawing technique have larger $d_c$ when $\phi$ is higher.

Generally, observing Figure 8, electrically drawn fibers (open symbols) can achieve higher rise in modulus compared to mechanically drawn fibers (solid symbols).
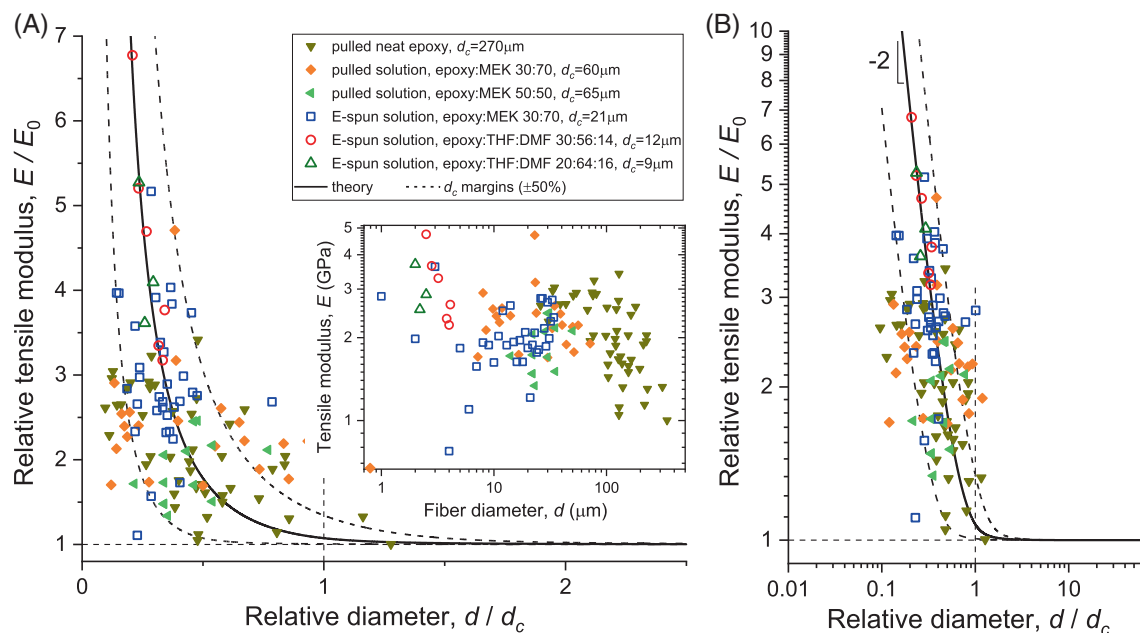
**FIGURE 8** Experimental evidence of fiber modulus diameter-dependence. The fibers were mechanically drawn (pulled, solid symbols) and electrically drawn (E-spun, open symbols) from neat resin or solution, at different compositions. The raw data are shown in the inset (log–log), of which the first group[5] and second and fourth groups[7] were published. The modulus $E$ is scaled by the bulk modulus $E_0$ (1 GPa for pulled fibers and 0.7 GPa for electrospun fibers). The fiber diameter $d$ is scaled by the critical diameter $d_c$ (or crossover diameter) approximated for each data group (see legend). The theoretical solution (solid curve, degree of polymerization $N = 10^3$, extent of reaction $p = 1/3$) is depicted for comparison (Equation 23), with ±50% margins (dashed curves) for $d_c$ uncertainty with respect to the gelation progress (Equation 28). (A) Liner plot. (B) Log–log plot.

This is primarily due to the higher strain rate achievable in the former technique, and the consequent smaller diameter (Equations 27 and 30), the subject of the next section. The achieved rise in modulus, which was up to about a factor of 7, is still far from the maximum possible theoretically, $\frac{E_{max}}{E_0} = \frac{E_1 p_c}{3 E_2/2}$ (Equations 22 and 23), which is in the order of 20–200 ($E_1/E_2 = 10^2 - 10^3$ and $p_c = 1/3$). This indicates that the clusters' molecular orientation in the tested fibers did not approach the maximum, possibly due to partial relaxation of stretched chains within the time gap between fiber deposition and final curing. Relaxation may be slowed down, for instance, by allowing a longer extent of reaction (larger $N$) prior to fiber processing (see Equations 7 and 8). Other tuning parameters may be applied as well, detailed in the next section. Further experiments may extend the fiber diameters to the sub-micron range, to achieve higher orientation and modulus rise.

## 3.3 | Mechanical and electrical drawing effects

The polymer molecular state under extensional flow is determined by the ratio between the flow strain rate $s$ and the critical strain rate $s_c = 3/\tau$ (Equation 14). $s_c$ is a solution property that depends on the monomer relaxation time $\tau_0$ and the degree of polymerization $N$ (or, equivalently, the relative extent of reaction $\varepsilon$). $s$ is a function of the applied extending stress $\sigma$ and the solution viscosity $\eta$ (Newton's law of viscosity):

$$s \approx \frac{\sigma}{\eta} \approx \frac{\sigma}{G(\tau)\tau}. \tag{32}$$

The viscosity of viscoelastic liquids is generally expressed by $\eta \approx G(\tau)\tau$, where $\tau$ is the relaxation time and $G(\tau)$ is Rouse relaxation modulus at that time.[26] The modulus in a liquid is high when a step strain is induced, and decays over time $t$ as the stress decays, and therefore it is defined as a function of time, $G(t)$. The characteristic time of the liquid is its relaxation time $\tau$, so that its characteristic modulus is $G(\tau)$. The relaxation modulus is of order $kT$ per polymer cluster, analogous to a polymer network of strands (that is, clusters) having entropic elasticity; the number density of clusters is proportional to $P/\xi_0^3$ where $P$ is the overlap parameter (the average number of clusters within the pervaded volume of a cluster) and $\xi_0$ is the cluster size (Equation 5).[26] As branched polymers near the gel point are space-filling but non-interacting, the overlap parameter in a neat resin is $P = \phi = 1$, that is no overlap. In a solution, solvent fills some of the space, and therefore $P$ is equal to the polymer

volume fraction $\phi$. Hence, the relaxation modulus is given by:

$$G(\tau) \approx \frac{\phi kT}{\xi_0^3} \approx \frac{\phi kT}{b^3 N^{3/\mathcal{D}}}. \tag{33}$$

The relative strain rate is:

$$\frac{s}{s_c} \approx s\tau \approx \frac{\sigma}{G(\tau)} \approx \frac{\sigma b^3}{\phi kT} N^{1.19}. \tag{34}$$

The result in Equation (34) can be used in the modulus equation to assess its parametric dependencies. Thus, the modulus approximate solution in Equation (24) can be written as:

$$E \approx \frac{2p_c E_0}{3(1-\epsilon_0)} \frac{\sigma b^3}{\phi kT} N^{1.19}, s \gg s_c, \tag{35}$$

where, $\epsilon_0$ is given by Equation (12). This equation summarizes the modulus rise dependence on the material and process parameters: monomer length $b$, polymer functionality $f$ and corresponding $p_c$ (Equation 1), solution concentration $\phi$, ambient temperature $T$, gelation (curing) state $N$ or $\varepsilon$, and applied stretching stress $\sigma$.

The applied stress $\sigma$ depends on the technique employed to produce the extensional flow, whether mechanical drawing (pulling)[5] or electrical drawing (electrospinning).[7,11,37] In electrical drawing, the density of the electric charge induced in the jet is proportional to the electric field intensity $E_\infty$ (not to be confused with the modulus), and therefore the electric shear stress acting on the jet surface far from the orifice is proportional to the electric field squared, $E_\infty^2$. Using dimensional analysis, we find that the electrospinning stress does not depend on the viscosity (surface tension neglected), and the scaling exponents of the other parameters can be derived:

$$\sigma_{\text{Espin}} \approx E_\infty^2 \left(\frac{\varepsilon_0 d_0 K}{v_0}\right)^{1/2}, \tag{36}$$

where, Espin stands for electrospinning, $\varepsilon_0$ is the permeability of free space, $d_0$ is the injector inner diameter, $v_0$ is the jet feed velocity, and $K$ is the solution electric conductivity. Other analyses yield slightly different exponents,[11,52,53] but with the same trends.

In typical mechanical drawing, the extension is applied by constant pulling velocity $v \gg v_0$ rather than constant force. In that case, the strain rate (assumed constant) is expressed by

$$s \approx \frac{v - v_0}{l} \approx \frac{v}{l}, \tag{37}$$

where, $l$ is the drawing distance. Using Stokes law, the force on a monomer of size $b$ scales as $\eta_r b \Delta v$, where $\eta_r$ is the resin or solvent viscosity, and $\Delta v = sb$ is the velocity difference along the monomer size. In terms of monomer stress, we have $\eta_r bsb/b^2 = \eta_r s$, and the average stress within the solution is $\eta_r s\phi$, proportional to the monomers area (volume) fraction. Using $s$ from Equation (37) we obtain the pulling stress at constant pulling velocity:

$$\sigma_{\text{Mpull}} \approx \frac{\eta_r \phi v}{l}, \tag{38}$$

where, Mpull stands for mechanical pulling. Substituting the stress expressions from Equations (36) and (38) in Equation (35), the parametric dependence of the modulus is obtained:

$$E \approx \frac{2p_c E_0 b^3 N^{1.19}}{3(1-N^{-0.28})kT} \begin{cases} \dfrac{E_\infty^2}{\phi}\left(\dfrac{\varepsilon_0 d_0 K}{v_0}\right)^{0.5} & \text{Espin} \\ \dfrac{v\eta_r}{l} & \text{Mpull} \end{cases} s \gg s_c, \tag{39}$$

where, $N$ may be expressed by the extent of reaction $\varepsilon$ (Equations 2–4). Interestingly, the electrospun modulus is independent of the spinning distance whereas the pulled modulus is independent of the concentration.

Similarly, the fiber diameter stress-dependence is (Equations 27, 32, 33, 7, and 8):

$$d \approx d_0\phi\left(\frac{v_0\eta_r}{\sigma l}\right)^{0.5} \begin{cases} N^{0.30} & \text{neat resin} \\ N^0 & \text{solution} \end{cases} s \gg s_c. \tag{40}$$

Unlike the modulus, the diameter is weakly dependent on the degree of polymerization. Substituting the stress expressions from Equations (36) and (38) in Equation (40), the parametric dependence of the diameter is obtained. For pulling it simply results in Equation (27), and for electrospinning of a solution it is given by:

$$d \approx \frac{d_0\phi}{E_\infty}\left(\frac{v_0\eta_r}{l}\right)^{0.5}\left(\frac{\varepsilon_0 d_0 K}{v_0}\right)^{-0.25} s \gg s_c. \tag{41}$$

The electrospun diameter is independent of the velocity whereas the pulled diameter is independent of the spinning distance.

These expressions provide a roadmap for tuning the material and process parameters to achieve desired fiber stiffness and diameter. For a given polymer type, the solution concentration (Figure 8), the temperature, and the extent of reaction[9] can be controlled. In electrical drawing, the applied field, the feedrate and the spinneret

diameter can be controlled,[7] as well as the solution conductivity by selection of solvents (Figure 8) and additives such as salt.[54] In mechanical drawing, the drawing velocity and distance may be controlled.[5] Generally, electrospinning has more tunable parameters, making it more amenable for high stiffness small diameter applications, as demonstrated in the epoxy fiber tests in Figure 8. Evidently, the stress in the extensional flow, driven by the electric field $E_\infty$ or the pulling velocity $v$, should be within the bounds that ensure formation of a continuous jet.[51]

# 4 | CONCLUSIONS

Thermoset polymer fibers such as epoxy microfibers exhibit a significant increase in stiffness, strength, and toughness at small diameters, making them likely candidates as components for structural applications. In this study, we described the molecular conformation of thermoset polymer solutions in extensional flow, and suggested a theoretical model to correlate the mechanical properties, specifically the stiffness (elastic modulus), with solution composition, extent of curing reaction, and flow conditions.

We have shown that two physical processes occur simultaneously—the hydrodynamic stretching of branched polymer molecules (clusters) and the narrowing down of the jet diameter. When the flow strain rate is faster than the polymer relaxation time, a conformational transition occurs, and the molecular extension becomes significantly high and stable. Cluster extension is accompanied by molecular orientation which results in stiffness increase in the solidified fully-cured fiber. The extension also rearranges the fiber's nodular structure in a sequential order, creating long chains of nodules. The correlation between stiffness and fiber diameter is expressed by an inverse-square power law, and the modulus rise transition point is characterized by a critical diameter, in agreement with experimental data. This correlation does not imply that the modulus depends directly on fiber diameter, but rather that the extensional flow affects both simultaneously.

Based on the model, we show how desired fiber stiffness and diameter may be achieved by tuning material and process parameters. Tuning optimization may have sustainability benefits in reducing material waste. The unique size-dependent behavior of thermoset fibers is not limited to stiffness, and we plan further theoretical investigation of the strength and toughness based on similar premises as for the stiffness.

## CONFLICT OF INTEREST STATEMENT
The authors declare no conflict of interest.

## ORCID
*Israel Greenfeld* https://orcid.org/0000-0001-9683-7267
*Mark Shneider* https://orcid.org/0000-0001-6027-4351
*Antonia Kaestner* https://orcid.org/0009-0005-7124-2001
*H. Daniel Wagner* https://orcid.org/0000-0002-0741-2169

## REFERENCES
[1] H. Dodiuk, S. H. Goodman, *Handbook of Thermoset Plastics: Introduction*, 3rd ed., William Andrew Inc, New York **2014**, p. 1.
[2] C. May, *Epoxy Resins: Chemistry and Technology*, Marcel Dekker, New York **1988**.
[3] J. C. Capricho, B. Fox, N. Hameed, *Polym. Rev.* **2020**, *60*, 1.
[4] X. Wang, W. J. Zhang, D. G. Yu, X. Y. Li, H. Yang, *Macromol. Mater. Eng.* **2013**, *298*, 664.
[5] X. M. Sui, M. Tiwari, I. Greenfeld, R. L. Khalfin, H. Meeuw, B. Fiedler, H. D. Wagner, *eXPRESS Polym. Lett.* **2019**, *13*, 993.
[6] N. Aliahmad, P. K. Biswas, V. Wable, I. Hernandez, A. Siegel, H. Dalir, M. Agarwal, *ACS Appl. Polym. Mater.* **2021**, *3*, 610.
[7] M. Shneider, X. M. Sui, I. Greenfeld, H. D. Wagner, *Polymer* **2021**, *235*, 235.
[8] X. Sui, I. Pinkas, H. D. Wagner, *Polymer* **2021**, *230*, 124034.
[9] M. Shneider, R. Zattelman, A. Kaestner, I. Greenfeld, H. D. Wagner, *J. Appl. Polym. Sci.* **2023**, *140*, 1.
[10] M. Richard-Lacroix, C. Pellerin, *Macromolecules* **2013**, *46*, 9473.
[11] I. Greenfeld, X. M. Sui, H. D. Wagner, *Macromolecules* **2016**, *49*, 6518.
[12] P. G. de Gennes, *Scaling Concepts in Polymer Physics*, Cornell University Press, Ithaca, N.Y **1979**, p. 324.
[13] M. Doi, S. F. Edwards, *The Theory of Polymer Dynamics*, The Clarendon Press, Oxford University Press, New York **1986**.
[14] D. S. Pearson, A. D. Kiss, L. J. Fetters, *J. Rheol.* **1989**, *33*, 517.
[15] H. Watanabe, *Prog. Polym. Sci.* **1999**, *24*, 1253.
[16] G. Ianniruberto, G. Marrucci, *J. Rheol.* **2001**, *45*, 1305.
[17] G. H. McKinley, T. Sridhar, *Annu. Rev. Fluid Mech.* **2002**, *34*, 375.
[18] P. K. Bhattacharjee, D. A. Nguyen, G. H. McKinley, T. Sridhar, *J. Rheol.* **2003**, *47*, 269.
[19] R. S. Graham, A. E. Likhtman, T. C. B. McLeish, *J. Rheol.* **2003**, *47*, 1171.
[20] I. Greenfeld, A. Camposeo, A. Portone, L. Romano, M. Allegrini, F. Fuso, D. Pisignano, H. D. Wagner, *ACS Appl. Nano Mater.* **2022**, *5*, 3654.
[21] D. W. Mead, R. G. Larson, M. Doi, *Macromolecules* **1998**, *31*, 7895.

[22] L. A. Archer, *J. Rheol.* **1999**, *43*, 1617.

[23] V. R. Mhetar, L. A. Archer, *J. Polym. Sci. Part B: Polym. Phys.* **2000**, *38*, 222.

[24] S. L. Shenoy, W. D. Bates, H. L. Frisch, G. E. Wnek, *Polymer* **2005**, *46*, 3372.

[25] Y. H. Wen, C. C. Hua, *J. Rheol.* **2009**, *53*, 781.

[26] M. Rubinstein, R. H. Colby, *Polymer Physics*, Oxford University Press, Oxford, New York **2003**; p. xi, 440 p.

[27] P. J. Flory, *Am. Chem. Soc.* **1941**, *63*, 3083.

[28] N. Lahlali, J. Dupuy, M. Dumon, *E-Polymers* **2006**, *79*, 1.

[29] Z. He, W. Lv, G. Gao, Q. Yin, *Polym. J.* **2022**, *54*, 1445.

[30] R. J. Silbey, R. A. Alberty, G. M. Bawendi, *Physical Chemistry*, 4th ed., John Wiley&Sons, Inc, Cambridge **2005**.

[31] B. H. Zimm, W. H. Stockmayer, *J. Chem. Phys.* **1949**, *17*, 1301.

[32] R. Everaers, A. Y. Grosberg, M. Rubinstein, A. Rosa, *Soft Matter* **2017**, *13*, 1223.

[33] C. P. Lusignan, T. H. Mourey, J. C. Wilson, R. H. Colby, *Phys. Rev. E* **1995**, *52*, 6271.

[34] J. E. Martin, D. Adolf, J. P. Wilcoxon, *Phys. Rev. A Gen. Phys.* **1989**, *39*, 1325.

[35] SIR-Industriale, *Epoxy Resins*, Chemira GmbH, Lachen **2023**.

[36] A. Kastanek, S. Podzimeka, J. Dostal, Simek, M. Bohdanecky, *Polymer* **2000**, *41*, 2865.

[37] I. Greenfeld, K. Fezzaa, M. H. Rafailovich, E. Zussman, *Macromolecules* **2012**, *45*, 3616.

[38] M. Daoud, P. Pincus, W. H. Stockmayer, J. Thomas Witten, *Macromolecules* **1983**, *16*, 1833.

[39] U. T. Kreibich, R. Schmid, *J. Polym. Sci., Polym. Symp.* **1975**, *53*, 177.

[40] K. Dusek, J. Plestil, F. Lednicky, S. Lunak, *Polymer* **1978**, *19*, 393.

[41] J. Mijovic, J. A. Koutsky, *Polymer* **1979**, *20*, 1095.

[42] C. M. Sahagun, S. E. Morgan, *ACS Appl. Mater. Interfaces* **2012**, *4*, 564.

[43] R. G. C. Arridge, *Mechanics of Polymers*, Oxford, UK, Clarendon Press **1975**; p. ix, 246 p.

[44] I. M. Ward, J. Sweeney, *An Introduction to the Mechanical Properties of Solid Polymers*, 2nd ed., Wiley, Chichester, West Sussex, England **2004**; p. x, 382 p.

[45] F. Ashby, D. R. H. Jones, *Engineering Materials 1: An Introduction to Properties, Applications and Design*, Butterworth-Heinemann, Oxford **2011**, p. 496.

[46] M. F. Ashby, *Materials Selection in Mechanical Design*, 4th ed., Elsevier, Burlington **2011**.

[47] M. F. Ashby, H. Shercliff, D. Cebon, *Materials: Engineering, Science, Processing and Design; North American Edition*, 3rd ed., Butterworth-Heinemann, Oxford **2013**.

[48] J. C. Slater, *J. Chem. Phys.* **1964**, *41*, 3199.

[49] Wolfram Periodic table – elements. https://periodictable.com/index.html

[50] M. Piggott, *Load Bearing Fibre Composites*, 2nd ed., Kluwer Academic Publishers, Dordrecht **2002**, p. 475.

[51] I. Greenfeld, E. Zussman, *J. Polym. Sci. Part B: Polym. Phys.* **2013**, *51*, 1377.

[52] F. J. Higuera, *J. Fluid Mech.* **2006**, *558*, 143.

[53] S. N. Reznik, E. Zussman, *Phys. Rev. E* **2010**, *81*, 026313.

[54] X. M. Sui, E. Wiesel, H. D. Wagner, *J. Nanosci. Nanotechnol.* **2011**, *11*, 7931.

## APPENDIX A: EXTENSION AND ORIENTATION FULL SOLUTION

This appendix provides full mathematical solutions for the extension and orientation.

### A.1. | Extension

Substituting the tension force (Equation 11) into the stretching equation (Equation 10):

$$3\epsilon \frac{1 - \epsilon_0}{1 - \epsilon} - 3\epsilon_0 \approx s\tau\epsilon, \tag{A1}$$

and solving the quadratic equation, the cluster relative extension as a function of the strain rate is obtained[20]:

$$\epsilon \approx \frac{1}{2}\left[\left(1 - \frac{3}{s\tau}\right) + \sqrt{\left(1 - \frac{3}{s\tau}\right)^2 + \frac{12\epsilon_0}{s\tau}}\right]. \tag{A2}$$

Approximations yield $\epsilon \approx \epsilon_0[1 + (1 - \epsilon_0)s\tau/3]$ for low $s\tau$ and $\epsilon \approx 1 - 3(1 - \epsilon_0)/s\tau$ for high $s\tau$. Note that $\epsilon_0$ is not negligible in a branched polymer; for example, for $N = 10^3$, $\epsilon_0 \approx N^{-0.28} \cong 0.15$ (Equation 12). By comparison, in a free linear chain with the same degree of polymerization, $\epsilon_0 \approx N^{-0.41} \cong 0.06$.

### A.2. | Orientation

Given a force $F_i$ acting on a monomer in direction $i$, and the corresponding normalized force $f_i = F_i b/kT$, the statistical Boltzmann factor is $e^{-F_i b/kT} = e^{-f_i}$. Thus, the probability that a monomer will align in direction $i$ is given by[11,20]

$$P_i^{\pm} = \frac{e^{\mp f_i}}{2Q}, i = x, y, z. \tag{A3}$$

The partition function in the denominator, $Q = \sum_i \cosh f_i = \cosh f + 2\cosh f_0$, ensures that the sum of

all alignment probabilities equals unity. The stretching force in the longitudinal direction $x$ is $f_x = f(\varepsilon) = f$, and in the lateral directions it is approximately the same as at rest $f_y = f_z = f(\varepsilon_0) = f_0$. The monomer alignment probabilities are:

$$P_x^{\pm} = e^{\mp f}/2Q$$
$$P_y^{\pm} = P_z^{\pm} = e^{\mp f_0}/2Q. \tag{A4}$$

Therefore, the relative extension is (Equation 16):

$$\epsilon = P_x^+ - P_x^- = \frac{\sinh(-f)}{Q} = \frac{\sqrt{\cosh^2 f - 1}}{\cosh f + 2\cosh f_0}, \tag{A5}$$

and at rest:

$$\epsilon_0 = \frac{\sqrt{\cosh^2 f_0 - 1}}{3\cosh f_0}. \tag{A6}$$

At the initial low tension $\epsilon_0 \approx f_0/3$, and at high tension $\varepsilon \to 1$, in agreement with Equation (11). The orientation in a cluster is given by (Equation 15):

$$O_s = \frac{3}{2}\left(P_x^+ + P_x^-\right) - \frac{1}{2} = \frac{\cosh f - \cosh f_0}{\cosh f + 2\cosh f_0}. \tag{A7}$$

Extracting $\cosh f$ and $\cosh f_0$ from Equations (A5) and (A6) in terms of $\epsilon$ and $\epsilon_0$, and substituting in Equation (A7) and rearranging, the overall molecular orientation is obtained as a function of the cluster relative extension[11,20]:

$$O = \frac{-\left(1 - 3\epsilon_0^2\right) + \sqrt{(1 - 9\epsilon_0^2) + 3(1 + 3\epsilon_0^2)\epsilon^2}}{1 + 3\epsilon_0^2} p_c, \tag{A8}$$

where, $\epsilon$ is given by Equation (A2), and the cluster weight fraction $p_c$ is added (Equation 17). Approximations yield $O \approx \epsilon_0^2 s\tau \frac{1 - \epsilon_0}{1 - 3\epsilon_0^2} p_c$ for low $s\tau$ and $O \approx \left[1 - \frac{9(1 - \epsilon_0)}{2s\tau}\right] p_c$ for high $s\tau$.